Novel Synthesis Zero -Valent Iron Nanoparticles for Removal alizarin red dye from aqueous Solution

F.M. El-Naggar, N.M. Ali, M. M.Moustafa and E.H. El-Mossalamy
Chemistry Dept., Faculty of Science, Benha Univ., Benha, Egypt.
E-mail: Fatma_chem27@yahoo.com

Abstract

Water pollution has become one of the most serious matters of concern in today's era of high industrial and technological advancement. Synthesized of Nano - scaled zero valet iron (nZVI) was in ethanol medium by reduction of ferric iron with different counter ions nitrate and chloride using sodium borohydride as a reducing agent under Nitrogen atmospheric conditions. The systematic Iron nZVI was performed using UV, XRD, SEM, EDX and BET studies.

The laboratory synthesized nZVI particles were examined for removal efficiency alizarin red dye from aqueous solution with different application adsorption isotherm; Langmuir, Freundlich and Temkin respectively.

Key Words: nZVI, NaBH$_4$, Alizarin red dye, XRD, UV, SEM and BET

1. Introduction

In today's era of tremendous industrial and technological advancement, water pollution has become one of the most important issues of concern. The discharge of industrial, agricultural, domestic, and municipal waste effluents into water bodies has resulted in a higher flow of toxic contaminants. Plants, animals, and humans are all affected differently by diverse types of contaminants [1, 2].

The use of zero-valent iron nanoparticle technology for the treatment of hazardous and toxic wastes, as well as the remediation of contaminated sites, is becoming increasingly popular. Since 2001, more than 20 projects have been completed in the United States alone. In North America, Europe, and Asia, more is planned or underway. The iron nanoparticles' small size aids in efficient subsurface dispersion, while their high specific surface area corresponds to increased relativity for rapid contaminant transformation. Recent advancements in nanoparticle synthesis and production have resulted in significant cost savings and increased availability of nanoscale zero-valent iron (nZVI) for large-scale applications. The methods of nZVI production and characterization are highlighted in this paper. The process of removing alizarin red dye is examined.

Nano-gold particles (10 nm) have been employed as molecular delivery carriers because they have a strong affinity for several functionalized species, including amino and nuclei aids. Gold nanoparticles function as intracellular gene regulation agents for the control of protein expression in ells when functionalized with oligonucleotides [3]. Furthermore, titania nanoparticle chemical stability, optical characteristics, and photochemical reactivity are significantly superior to their conventional mircoscale counterparts [4]. Titania nanoparticles

have been considered as being more suited for photoelectrical energy conversion and photocatalysis. At the nanoscale, materials' energy and electronic properties are discrete rather than continuous, as they are in bulk materials.

Many research papers on nZVI synthesis in aqueous medium have been published in recent years. However, the formation of iron nanoparticles in ethanol medium has not been fully studied. Hence, the goal of this study is to synthesis nZVI in the open air in the presence of ethanol in order to prevent major oxidation and to characterize the synthesized materials in terms of their surface characteristics and size [5]. We manufactured and characterized iron-based nanosale particles with zero oxidation state in this study. The materials were characterized using an X-Ray diffraction (XRD) and a scanning electron microscope (SEM) with energy-dispersive X-ray spectroscopy (EDX), ultraviolet–visible spectroscopy (UV-VIS), and a surface area (BET).

2. Materials and methods

2.1. Materials

Ferric chloride unhydrous (FeCl3), Ferric nitrate [Fe (NO3)3.9H2O], Sodium borohydride (NaBH4) and alizarin red dye were purchased from Sigma–Aldrich chemical company and were used without further refinement. All other reagents were analytical reagent grade. Throughout the research, deionized water was used.

2.2. Preparation of nZVI particles

The iron nanoparticles were made in an ethanol flask reactor with three open necks, as shown in (Fig. 1). The reaction is as follows:

$$2FeX_n + 6NaBH_4 + 18H_2O \rightarrow 2Fe^0 + 6NaX + 6B(OH)_3 + 21H_2 \qquad (1)$$
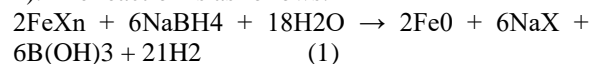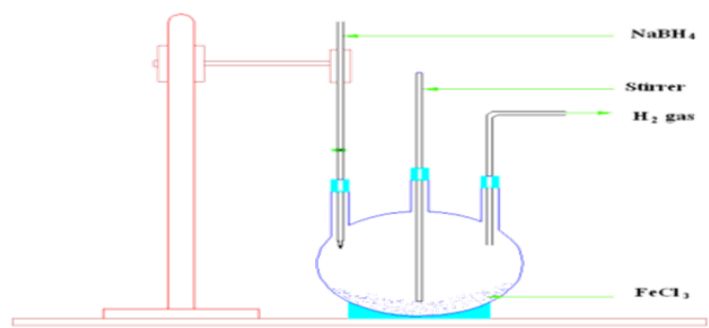
Fig. (1) Schematic diagram for synthesis of iron nanoparticles.

To prepare nanoscale Zero Valent Iron (nZVI) [X(Fe0/Cl⁻)] and [Y(Fe0/NO3–) from different anions such as chloride (Cl⁻) and nitrate (NO3–), a 0.6 M solution of each salt was dissolved in a 4/1 (v/v) ethanol/water mixture (24 ml ethanol+6 ml deionized water) and stirred well. On the other hand, a 0.8 M sodium borohydride solution was made by dissolving 3.028 g NaBH4 in 100 ml deionized water; excess borohydride is required for better growth of iron nanoparticle. The borohydride solution is poured into a burette and added to each solution drop by drop (1 drop per 2 seconds) while vigorously stirring. Immediately after the first drop of sodium borohydride solution, black solid particles emerged, and the remaining sodium borohydride solution was added completely. After adding the entire borohydride solution, the mixture was stirred for another 30 minutes. The black iron nanoparticles were separated from the liquid phase using the vacuum filtration technique. To eliminate all of the water, the solid particles were rinsed three times with 25 mL portions of absolute ethanol. Because it avoids the quick oxidation of zero valent iron nanoparticle, this washing procedure is likely the most important stage in the production. After that, the precipitate was placed in an autoclave at 160℃ for 4 hours. Finally, the produced nanoparticles were dried overnight at 60℃. A thin layer of ethanol was applied to protect the nano iron particles from oxidation during storage.

2.3. Adsorption experiments

The batch experiment approach was used to determine alizarin red dye adsorption onto nZVI. The effects of contact time, alizarin red dye initial concentration, pH, nZVI dosage, ionic strength, and temperature were investigated using protocol as follows: 50 mL of dye solution with known initial concentration (150 mg/L) was shaken with a specific amount of adsorbent (0.001 g) on a horizontal shaker at 400 rpm at the default pH. The time was changed from 10 to 240 minutes. To measure the level of color removal, sample solutions were taken out at predefined time intervals. At 303, 308, and 313 K,

the effect of temperature on alizarin red dye adsorption was examined using optimal contact time (180 min for X and 120 min for Y) and nZVI dosage (0.01 g). Samples were removed from the conical flasks after each predetermined time interval, and the alizarin red dye solutions were separated from the adsorbent by filtration, which was followed by centrifugation. A Jaso UV-Vis spectrophotometer (Jaso; model V 670) was used to evaluate the residual dye concentration in the supernatant solutions at the Chemistry Department, Faculty of Science, Benha-University. The formula [6] was used to calculate the percentage removal of alizarin red dye by nZVI:

$$R (\%) = (c_i-c_f)/c_i \times 100 \qquad (2)$$

Where ci and cf are the initial and final alizarin red dye concentration before and after adsorption (mg/L); R (%) is the alizarin red dye removal efficiency (%).
The adsorption capacity of alizarin red dye on nZVI was determined using the following equation [7]:

$$q = ((c_o-c_e) \times V)/W \qquad (3)$$

Where co and ce are the initial and given time alizarin red dye concentrations (mg/L), respectively, q is the quantity of alizarin red dye adsorbed per unit mass of nZVI (mg/g), V is the volume of alizarin red dye solutions (L) and W is the weight of sorbent (g).

2.4. Characterization tools and equipment

2.4.1. Powder X-ray diffractometer

The synthesized products were measured using x-ray powder diffraction, 18 KW diffractometer (Bruker; model D 8 advance) with monochromatic cu-Ka radiation, 1.54178 (Ao). The crystallinity and phase purity of the as-prepared nanomaterials were determined using an X-ray diffraction. At room temperature, the diffraction patterns were reordered in the angular range of 30o-90o (2 Ө), with a step size of 0.02o (2 Ө), and a san step time of 0.4. (s). This was carried out at Cairo, Egypt's central Metallurgical R and D Institute.

2.4.2. Field emission scanning electron microscope (FE-SEM)

The morphology and elemental composition of the as-prepared nanomaterials were investigated using Field emission scanning electron microscope (SEM,

JEOL JSM-6510LV) joined with energy dispersive x-ray spectroscopy (EDX, Oxford Instruments, Model No: 7582) operating at an accelerating voltage of 20 KV. The (FE-SEM) and gold coating process by using EMITECH K550X sputter coater. This was performed at agriculture faculty, Mansoura University, Egypt.

2.4.3. Ultraviolet-visible spectroscopy (UV-Vis)

The UV–Vis spectrum of Fe0 nanoparticles was recorded using UV–Vis spectrophotometer, at the range of 200-600 nm at chemistry Department, Faculty of Science, Benha University.

2.4.4. BET surface area

The various surface parameters of the prepared nZVI were determined from N2 adsorption-desorption isotherms measured at -196°c using BELSORP max II equipment, Japan. The samples were initially out-gassed under vacuum (10-4 Torr) at 300°c for 1h. BET surface areas (SBET) were calculated by the aid of BET equation at EPRI, Cairo, Egypt.

3. Results and discussion

3.1.Characterization of synthesized nZVI particles

(Fig. 2a, 2b) show the XRD examination of X and Y nanoparticles, respectively. The peak at 2θ 44.87o and 44.68o, respectively, which represents 100 % intensity, indicates the presence of α-Fe0 nanoparticles in the sample for X and Y nanoparticles. The (X and Y) nanoparticles' mean crystalline dimensions were found to be 3.166 and 1.83 nm, respectively. Other investigations [8, 9] yielded similar results.

FE-SEM (Fig. 3) and (Fig. 4) are used to examine the particle size and morphology of the prepared nZVI (X and Y samples) at various magnifications. Figure

3(a-d) shows FE-SEM images of generated nZVI nanoparticle images. The presence of ultrafine and crystalline spherical forms with aggregation may be seen in the images. The magnetic dipole–dipole interactions and huge surface area of the individual particles are said to cause iron nanoparticle aggregation. SEM images were used to determine the average particle size of the nZVI nanoparticles (X sample), which was found to be in the range of 50-100 nm. The determined size is larger than the estimated size from the XRD pattern, implying that the appearance of the fine particles colliding with each other as densification. The EDX technique was used to evaluate the elemental analysis of (X sample) (Fig. 3i). As demonstrated in (Fig. 3) and (Fig. 4), the EDX spectrum displays a signal in the iron region, confirming the synthesis of nZVI (Fig. 4). In addition, SEM pictures (fig. 3(e-h)) demonstrate the crystalline spherical network morphologies for (Y), with average particle sizes in the range of 50-100 nm. The elemental analysis of the (Y sample) using the EDX instrument (Fig. 3j) shows a signal in the iron region, confirming the synthesis of nZVI.

For a spherical particle with a diameter of d, the specific surface area (SSA) can be calculated by the following equation:

$$SSA = (Surface\ Area)/Mass = 〚\pi d〛^2/(\rho\ \pi/6\ d^3) = 6/\rho d \qquad (4)$$

Where (ρ) is the density (7,800 kg/m3 for iron) of the solid particle. The BET measurements of surface area analyzer yielded SSA values 6,840 m2/kg and 10,300 m2/kg for (Y and X) respectively.
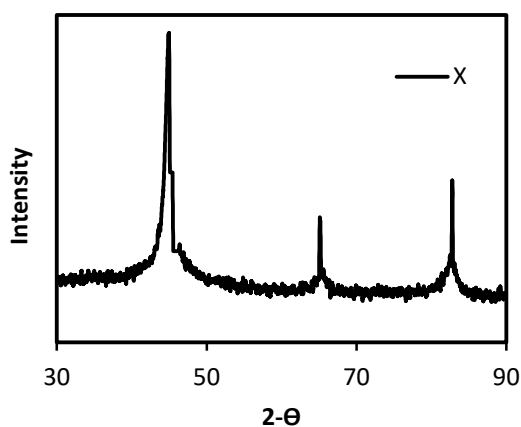
Fig. (2a) X-ray diffraction (XRD) pattern of X.
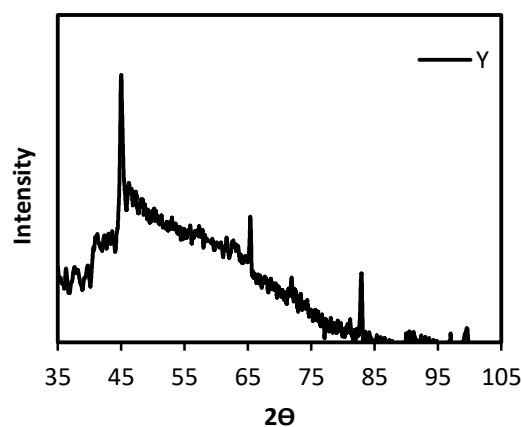
Fig. (2b) X-ray diffraction (XRD) pattern of Y.
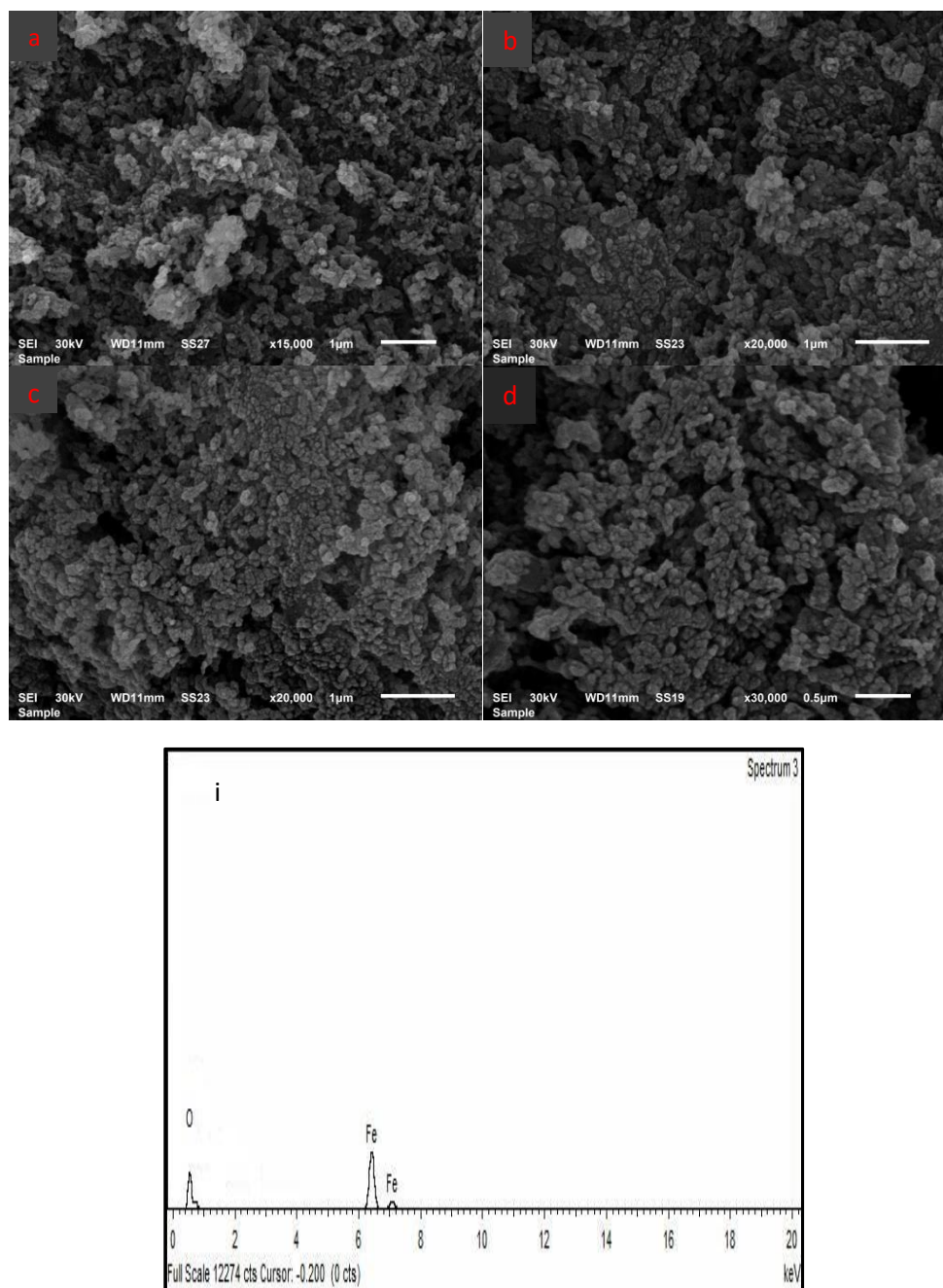
Fig. (3) FE-SEM images of the nZVI nanoparticles (X (a-d), sample) and EDX pattern (i (X)).
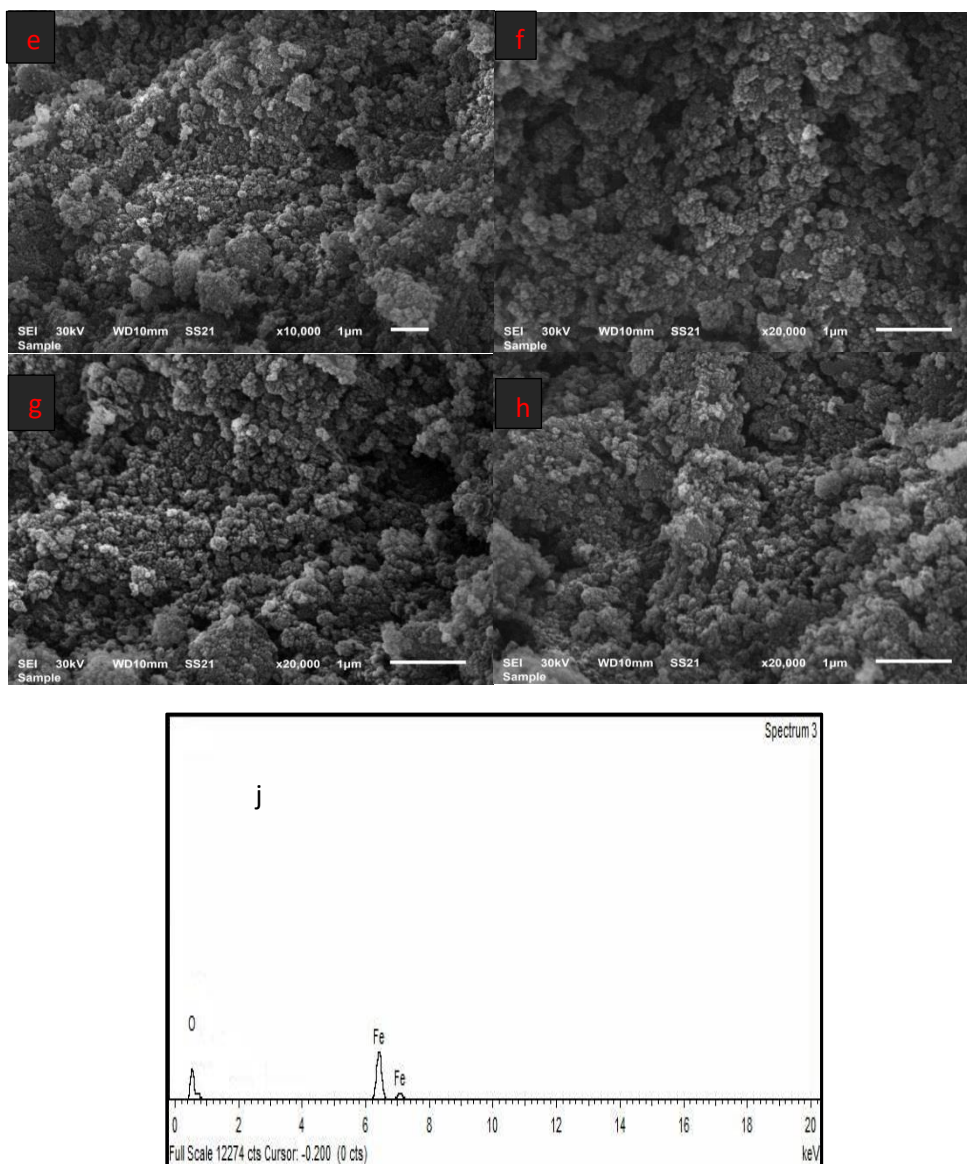
Fig. (4) FE-SEM images of the nZVI nanoparticles (Y (e-h), sample) and EDX pattern (j (Y)).

3.2. Adsorption studies
3.2.1. Adsorption of alizarin red dye on X and Y nanoparticles
3.2.1.1. Effect of initial pH

One of the most important variables in controlling the adsorption process, particularly the adsorption capacity, is the pH of the adsorbate solution. In the pH range of 3-9, the effect of initial pH on the removal of 150 mg/L of alizarin red dye by using 0.001g of (X and Y) samples was investigated. For all samples, the removal dye efficiency was calculated as shown in (Fig. 5). At pH = 3, the removal dye efficiency reordered at λ_{max} =590 nm, with maximum values (87.75 % for X) and (43.52 % for Y). The removal efficiency then reversed the

decreasing trend by lowering the pH levels in all of the samples under investigation.

3.2.1.2. Effect of contact time

One of the most important factors affecting the performance of adsorption processes is the contact time between adsorbate and adsorbent. At pH 3, 0.01 g adsorbent dosage, and initial alizarin red dye concentration of 150 mg/L, the effect of contact time of (X and Y samples) on the adsorption of alizarin red dye was examined. (Fig. 6) illustrates the alizarin red dye adsorption capacities of synthesized adsorbents as a function of stirring times ranging between 10-240 min for (X) and 10-180 min for (Y). The rate of uptake was rapid at first, and then gradually increased in the later stages until it reached

saturation, as shown in (Fig. 6). The maximum alizarin red dye removal was achieved in (180 minutes for X) and (120 min for Y).

3.2.1.3. Effect of initial dye concentration

The effect of varying the starting quantity of alizarin red dye from 50 to 350 mg/L on (X and Y samples) was studied. These adsorption studies were carried out with a pH of 3 and a dosage of 0.01 g adsorbent. The adsorbent was separated by centrifugation after (180 min for X) and (120 min for Y) of stirring, and the residual dye concentration in the supernatant was determined using UV-Vis spectrophotometric. The rate of uptake was high at first and quickly approached saturation. As time passed, the active sites were blocked, and the rate fell, as indicated in (Fig. 7). (Fig. 7) exhibited the relation between the initial dye concentration and the adsorption capacity. From (Fig. 7), the adsorption capacities increased with increasing the initial concentration until reached the maximum and constant high initial concentrations. From the data, the adsorption capacities of (X and Y samples) were determined to be 139.029 and 99.416 mg/g.

3.2.1.4. Effect of adsorbent dose

One of the most important parameters that determines the adsorbent's capacity for a given initial adsorbate concentration is the adsorbent dosage. Using various doses of adsorbent (0.001–0.01 g), the effect of adsorbent dosage on the adsorption of alizarin red dye was investigated. At equilibrated time, the adsorbent was added to 50 mL of alizarin red dye solutions with initial concentrations of 150 mg/L for (X and Y). After the solutions had reached equilibrium, they were centrifuged and tested for dye content. The adsorption results are depicted in (Fig. 8). Because the adsorbent surface active size grows, the results suggest that increasing the adsorbent dosage increases dye removal efficiency. The maximum alizarin red dye removal percentages for

(X and Y samples) were found to be 92.786 % and 85.206 %, respectively.

of the boundary layer enclosing the sorbent decreases. The adsorbate mass transfer resistance in the boundary layer decreased. This could have occurred as a result of an increase in the dye's mobility (owing to an increase in kinetic energy) as the temperature rose. The removal percentage of the alizarin red dye over the fabricated samples increased as the temperature of the dye solution decreased.

3.2.1.5. Effect of ionic strength

One of the most important variables that control both electrostatic and non-electrostatic interactions between the adsorbate and the adsorbent surface is the ionic strength of the dye solution. Using 0.01 to 0.1 g of NaCl salt at constant dye concentrations of 150 mg/L for X and Y at pH=3 and room temperature (30°C), the effect of NaCl on the adsorption of 0.01 g of alizarin red dye over X and Y adsorbents was studied. The effect of ionic strength (NaCl salt) on adsorption ability was demonstrated in (Fig. 9). From the extracted data, the ionic strength (dosage of NaCl) increases, however the percentage of alizarin red dye removal efficiency decreases due to decreasing surface charge in the dye solution.

3.2.1.6. Effect of temperature

The temperature factor has a significant impact on the rate of adsorption process. Adsorption studies for alizarin red dye removal were carried out at three different temperatures (303, 308, and 313 K) using 0.01 g of (X and Y adsorbents) and dye concentration of 150 mg/L for X and Y. As shown in the experimental data, the removal percentage increased slowly as the solution temperature increased for alizarin red dye (Fig. 10). This indicates that the alizarin red dye adsorption on the prepared adsorbents is an endothermic process. The results suggest that when the temperature rises, the thickness
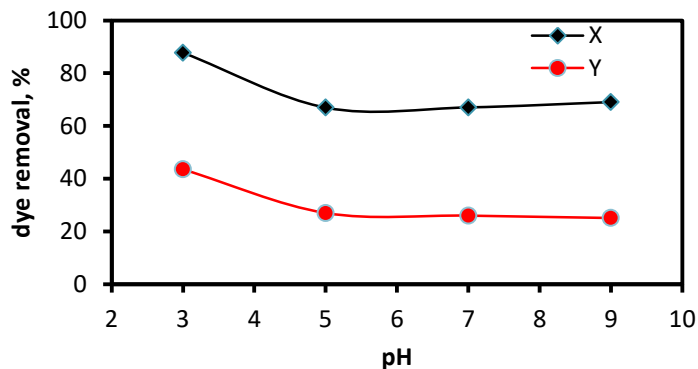
Fig. (5) Effect of initial pH on the removal of alizarin dye on X and Y samples.
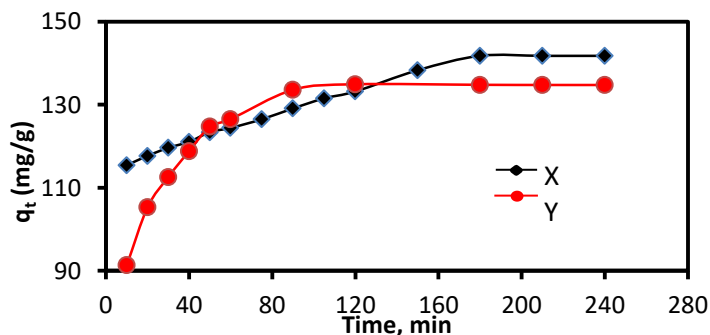
Fig. (6) Effect of contact time on the adsorption capacities of X and Y adsorbents for the removal of alizarin red dye.
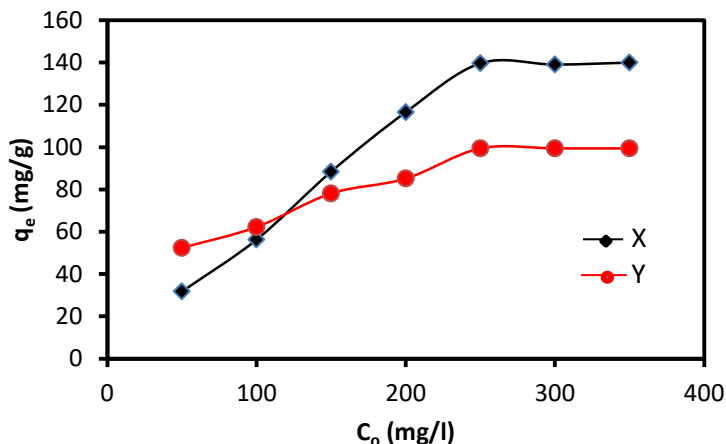
Fig. (7) Effect of initial alizarin red dye concentration on adsorption capacities of X and Y adsorbents for the removal of alizarin red dye.
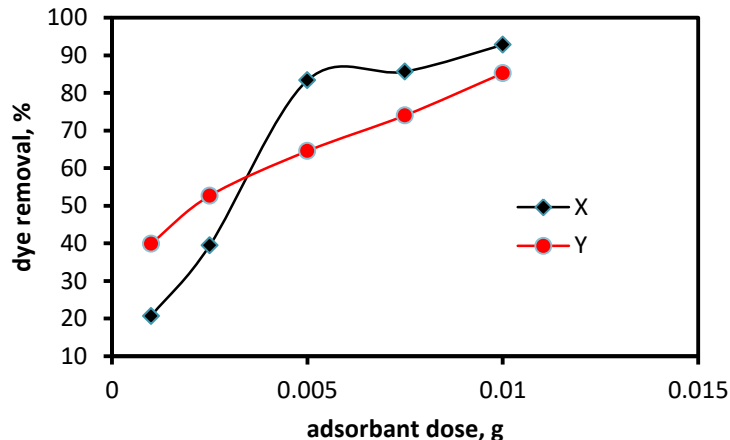
Fig. (8) Effect of adsorbent dose on the alizarin red dye removal efficiency using X and Y adsorbents.
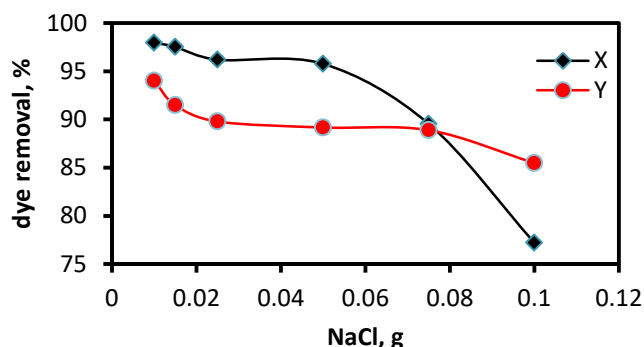
Fig. (9) Effect of NaCl amount on the alizarin red dye removal percentage using X and Y adsorbents.
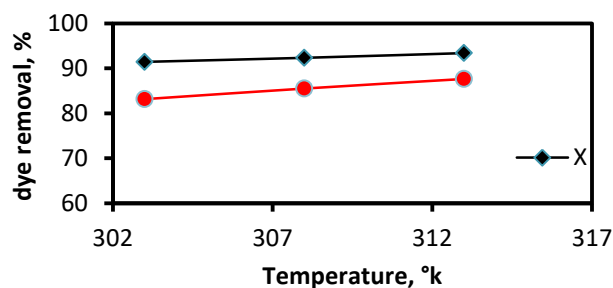
Fig. (10) Effect of temperature on the alizarin red dye removal percentage using X and Y adsorbents.

3.2.2. Adsorption isotherm studies

The most common isotherm models which show the experimental adsorption results carried out using different equilibrium concentration of alizarin red dye are Langmuir, Freundlich and Temkin.

3.2.2.1. Langmuir isotherm model

This model assumes that the dye molecules uptake occurs on a homogenous surface by monolayer without any interaction between adsorbed molecules [10]. Langmuir equation is expressed in the (equation No.5).

$$\frac{C_e}{q_e} = \frac{1}{K_L q_m} + \frac{C_e}{q_m} \qquad (5)$$

Where, C_e is the equilibrium concentration alizarin red dye in solution (mg/L) and q_e is the alizarin red dye equilibrium adsorption capacity on the (X and Y adsorbents). K_L is the Langmuir Constant (L/mg) which is related to the energy of adsorption. q_m is the adsorbed solute maximum quantity required to form adsorbent monolayer per gram (mg/g). Linear plot of C_e / q_e against C_e gave a

straight line for the Langmuir isotherm, as shown in (Fig. 11a, 11b). From the linear plots, the constants q_m and K_L can be calculated from the slope and intercept which are showed in Table (1). From R_L constant, The Langmuir isotherm essential characteristics can be expressed as shown in the (equation No. 6).

$$R_L = 1/(1 + K_L C_o) \qquad (6)$$

Where, K_L is the Langmuir constant and C_o is the initial dye concentration (mg/L). R_L value points out the adsorption nature to be unfavorable if $R_L > 1$, linear if $R_L = 1$, favorable if $0 < R_L < 1$ and irreversible if $R_L = 0$ [11]. From the data calculated in Table (1), The estimated adsorption capacity from Langmuir isotherm was determined to be 149.253 and 113.636 mg/g for the prepared samples under study (X and Y adsorbents) which are closed with the experimental values (139.634 and 99.416 mg/g). The R_L is greater than 0 but less than 1. It reflects that the adsorption of the alizarin red dye over the (X and Y adsorbents) is a favorable process.
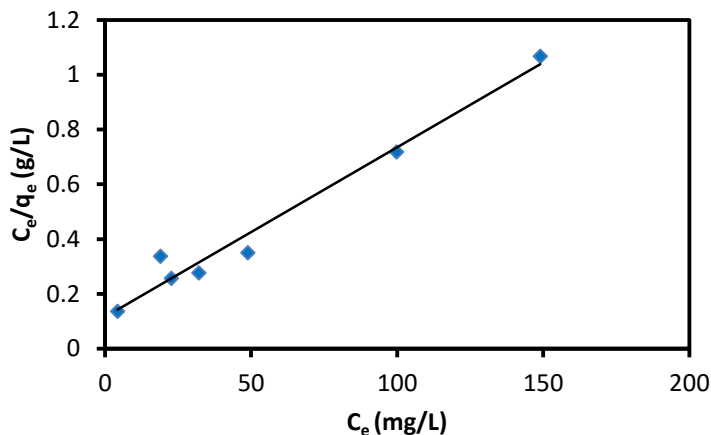
Fig. (11a) Langmuir isotherm for adsorption of alizarin red dye on X sample.
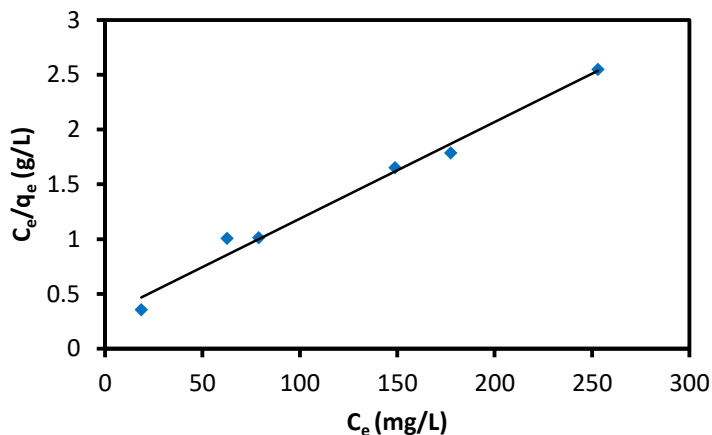
Fig. (11b) Langmuir isotherm for adsorption of alizarin red dye on Y sample.

3.2.2.2. Freundlich isotherm model

This isotherm model theory says that the mount ratio of solute adsorbed onto a given mass of sorbent to the concentration of the solute in solution is not constant at different concentrations. In addition to the heat of adsorption in magnitude decreases with increasing the adsorption extent [12]. The Freundlich linearized isotherm is expressed in the following relationship (equation No. 7, 8).

$$Lnq_e = LnK_f + \frac{1}{n} LnC_e \tag{7}$$

$$K_f = \frac{q_m}{c_o^{1/n}} \tag{8}$$

Where, K_f is the freundlich constant (mg/g) which represents the relative adsorption capacity of the (X and Y) adsorbent. (1/n) is the heterogeneity factor which is a function of the strength of adsorption in

the adsorption process. The linear plot between lnq_e verses lnC_e gives a slope which is equal to 1/n value and intercept is $\ln K_f$ as shown in (Fig. 12a, 12b) If n =1 then the partition between the two phases are independent of the concentration. If (1/n) value <1, it indicates a normal adsorption. On the other hand; if (1/n) >1, it indicates cooperative adsorption [13]. The linear least-squares method and the linearly transformed equations have been applied to correlate data of sorption where 1/n is a heterogeneity parameter, the smaller 1/n, the greater the expected heterogeneity. This expression reduces to a linear adsorption isotherm when 1/n = 1. If 1<n<10, this indicates a favorable sorption process. The extracted data are presented in Table (1). From extracted data, the samples were concluded in the n range of 2.2-3.6, this indicates a favorable sorption process.
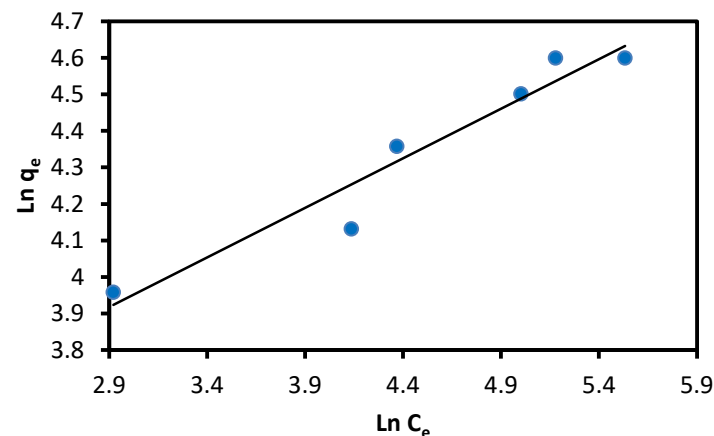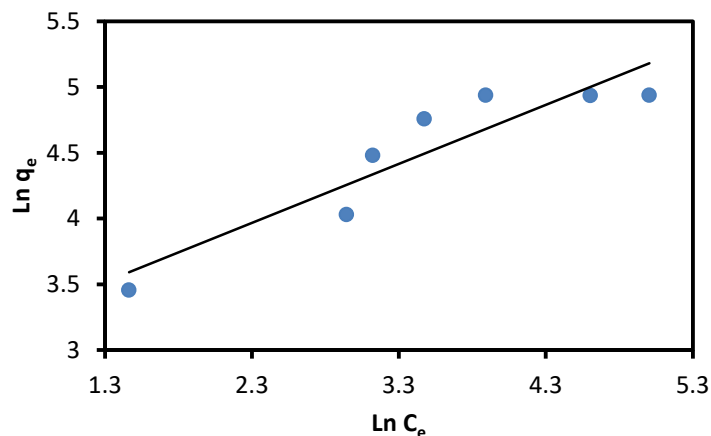
Fig. (12a) Freundlich isotherm for the adsorption of alizarin red dye on X sample.

Fig. (12b) Freundlich isotherm for the adsorption of alizarin red dye on Y sample.

3.2.2.3. Temkin isotherm model

Temkin isotherm model assumes that heat of adsorption of all molecules in the layer would decrease linearly rather than logarithmic with coverage due to the adsorbent–adsorbate repulsions and the adsorption of adsorbate is uniformly distributed [14, 15]. Temkin isotherm can be expressed in the following equation (equation No. 9, 10).

$$q_e = B\ln K_T + B\ln C_e \qquad (9)$$

$$B = \frac{RT}{b} \qquad (10)$$

The isotherm constants K_T is the equilibrium binding constant (L/mol) corresponding to the maximum binding energy and constant B is corresponding to the heat of adsorption [16]. q_e is the amount sorbed of metal ion in mg /g, C_e is

equilibrium concentration of the metal in solution in mg/ L, T is the temperature in kelvin, R is the universal gas constant (8.315×10^{-3} J mol^{-1} K^{-1}). The slope and intercept determines the isotherm constants from a plot of q_e versus $\ln C_e$ as shown in (Fig. 13a, 13b). The values of Temkin isotherm parameters are listed in Table (1). From the data of Temkin isotherm, the heat of adsorption (b) has values in the range of (73.39-126.89 J/mol) and it appears the weak interaction force between the surface of adsorbents and alizarin red dye. Besides, the K_T found to be in the range of (1.681-1.765 L/g) and the Temkin constant (B) value was in the range of (20.049-34.663 J/mol). The of Temkin equation R^2 value was in the range of (0.851-0.9168) for the synthesized samples under study (X and Y adsorbents) and it is lower than that obtained for the other isotherms.
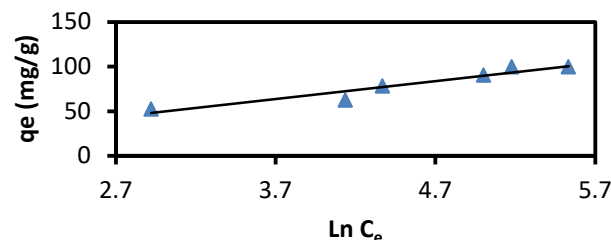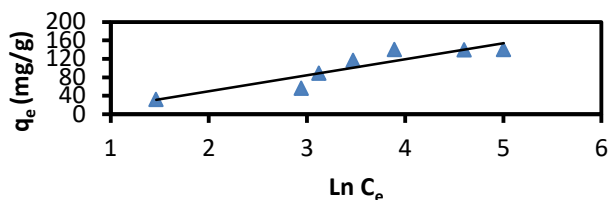
Fig. (13a) Temkin isotherm for the adsorption of alizarin red dye on X sample.

Fig. (13b) Temkin isotherm for the adsorption of alizarin red dye on Y sample.

Table (1) the extracted parameters from Langmuir, Freundlich and Temkin isotherms for X and Y adsorbent

Adsorption isotherm	Parameter	Values	
		X	Y
Langmuir parameters	KL (L/mg)	0.0754	0.0287
	qm (cal) (mg/g)	149.253	113.636
	RL	0.0474-0.2583	0.1037-0.4099
	R^2	0.9717	0.9851
	qm (exp) (mg/g)	139.634	99.416
Freundlich parameters	KF [(L/mg) (L/mg)$^{1/n}$]	12.611	22.899
	qm (cal) (mg/g)	150.382	102.362
	n (L/mg)	2.227	3.687
	R^2	0.8512	0.9279
	qm (exp) (mg/g)	139.634	99.416
Temkin parameters	KT (L/mg)	1.7659	1.6817
	b (J/mol)	73.394	126.893
	B	34.663	20.049
	R^2	0.851	0.9168

X is the nZVI prepared from ferric chloride and Y is the nZVI prepared from ferric nitrate.

4. Conclusions

Nanoscaled zero valent iron was prepared in the ethanolic medium by borohydride reduction method. Prepared nZVI characterization was achieved using XRD, SEM, UV and BET techniques. The results showed that nZVI exists mainly in the zero oxidation state with 100% intensity at 2θ of 44.87^o and 44.68^o for (X and Y) respectively, have mean crystalline size of 3.166 and 1.83 nm respectively and there was no oxidation during storage for weeks through visual observation. SEM results showed that nZVI appear as a spherical particle and take shape of chain-like structures with a particle size in the range 50-100 nm and that nZVI have a strong trend to agglomerate in nanoscale aggregates due to the weak surface charges. Prepared nZVI particles were used as an adsorbent for alizarin red dye removal from aqueous solutions. In UV-Visible, the results showed that percentage of removal was found to be 92.786 % and 85.206 % after 180 min and 120 min for (X and Y) respectively for alizarin red dye initial concentration of 150 mg/L. The adsorption data followed well the Langmuir isotherm model for all the prepared nZVI. The BET measurements of surface area analyzer yielded SSA values 6,840 m^2/kg and 10,300 m^2/kg for (Y and X) respectively.

References

[1] M.Yusuf, F.M. Elfghi, S.A.Zaidi, E.C.Abdullah and M.A.Khan, RSC Advances. vol.5, pp.50392, 2015.

[2] M.Ajmal, M.Siddiq, N.Aktas and, N.Sahiner, RSC Advances. vol.5, pp.43873–43884, 2015.

[3] N.L.Rosi, D.A.Giljohann, C.S.Thaxton, A.K.R.Lytton-Jean, M.S.Han, and C.A.Mirkin, Science. vol.312, pp.1027, 2006.

[4] D.G.Shchukin, J.H.Schattka, M.Antonietti, and R.A.Caruso, J.Phys. Chem. B. vol.107, pp.952, 2003.

[5] R.Yuvakkumar, V.Elango, V.Rajendran and N.Kannan, Digest Journal of Nanomaterials and Biostructures. vol.6, pp.1771, 2011.

[6] Ü.Geçgel, G.Özcan and G.Ç.Gürpınar, Journal of Chemistry, Article ID, 614083, 2013.

[7] J.Malina and A.Rađenović, Chemical and Biochemical Engineering Quarterly. vol.28, pp.491, 2015.

[8] M.R.Taha and A.Ibrahim, Journal of Environmental, 2014.

[9] J.Fan, Y.Guo, J.Wang and M.Fan, Journal of Hazardous Materials. vol.166, pp.904, 2009.

[10] S.Rizk and M.M.Hamed, kaolinite and tafla, Desalin. Water Treat. vol.56(6), pp.46, 2015.

[11] A.Dada, A.Olalekan, A.Olatunya and O.Dada, IOSR J.Appl. Chem. vol.3(1), pp.38, 2012.

[12] A.Agrawal, K.Sahu and B.Pandey, Colloids Surf. A. vol.237(1-3), pp.40, 2004.

[13] S.V.Moha and J.Karthikeyan, Environ. Pollut. vol.97(1), pp.7, 1997.

[14] I.V.Mishakov, A.F.Bedilo, R.M.Richards, V.V.Chesnokov, A.M.Volodin and V.I. Zaikovskii, J.Catal. vol.206(1), pp.8, 2002.

[15] R.Richards, R.S.Mulukutla, I.Mishakov, V.Chesnokov, A.Volodin and V.Zaikovski, Scr. Mater. vol.44(8), pp.6, 2001.

[16] X.Wang and Y.Qin, Biochem. vol.40(2), pp.80, 2005